(08) Seismic control effect of lattice grid structure with SMA spring-friction bearings

Zhuang Peng[1,2,a*], Wang Wenting[2,b]

[1] Beijing University of Civil Engineering and Architecture Beijing Higher Institution Engineering Research Center of Structural Engineering and New Materials, Beijing 100044, P. R. China

[2] School of Civil and Transportation Engineering, Beijing University of Civil Engineering and Architecture, Beijing 100044, P. R. China

[a]email: harryzhpeng@126.com, [b]email: waitings2014@sina.com

Key words: shape memory alloy (SMA); lattice grid structures; seismic isolation; superelasticity; helical spring

Abstract: A new type of seismic isolation device, SMA spring-friction bearing (SFB) is developed and its application to lattice grid structures is investigated in this paper. First, a simplified restoring model is derived to simulate the hysteretic behavior of the SFB. Then, a SFB specimen is fabricated and tested using cyclic protocol to validate the model of such an isolator. Finally, the feasibility and the seismic control effect of the SFB in the lattice grid roof with substructure are evaluated by performing a set of nonlinear time history analyses. The numerical results indicate that the SFB is effective in controlling displacement, roof acceleration and base shear of the lattice grid structures.

Introduction

Analytical studies, experimental works and construction applications have shown that seismic isolation technology is an effective way to improve the seismic performance of engineering structures. To develop high performance isolation control devices, several researchers have proposed the use of smart materials for structural control. Recently, there has been an increasing interest in utilizing superelastic SMA devices for the development of new seismic isolation systems [1-5]. Although the analytical and experimental studies have proven that the structures with superelastic SMA components usually in the form of wires and bars improve the seismic response, further research of large-scale SMA element is necessary to fully explore the possibility of applying SMA in the passive control of structures. Some researchers suggested the use of superelastic SMA helical spring instead of SMA wires or SMA bars as energy dissipation and re-centering control system. For example, Speicher et al. [6] developed a tension/compression damper making use of SMA helical springs, which provide stable re-centering and damping characteristics. Attanasi et al. [7] proposed conceptual design of an innovative restorable isolation system in which a sliding bearing is coupled with superelastic SMA helical springs that function for re-centering purposes.

From the application point of view, the large scale SMA helical springs can be used as re-centering and energy dissipation components for dampers and isolators. Most of the previous studies were focused on the development and application of SMA helical springs for isolation control of multi-story buildings. However, very few attempts have been given to the investigation of behavior of long span and spatial structures isolated by restorable isolation systems with large scale SMA helical springs. The primary objective of this study is to carry out an investigation on feasibility and efficiency of a new type of restorable friction isolator with SMA springs The

© 2015. The authors - Published by Atlantis Press

proposed isolator spatial structures, which is entitled as SMA spring-friction bearing (SFB), consists of a flat sliding bearing that decouples superstructures from horizontal ground motions by providing frictional sliding interfaces, SMA helical springs that provide re-centering mechanism and dissipate seismic energy through hysteresis effects. In this paper, the conceptual design and the functioning mechanism of the SFB are described. Then, a simplified theoretical model is derived to capture the overall response of the SFB. In order to investigate mechanical behaviors of the SFB, the experimental studies are carried out to verify the performance of the bearing. Finally, a set of nonlinear time history analyses using SAP2000 software are performed to examine the effectiveness of the developed isolator in reducing seismic response of lattice grid structures.

Conceptual design and working principle of the SFB

The SFB device primarily consists of two parts: (i) a horizontal sliding isolation bearing, (ii) large diameter SMA helical springs. Apart from the friction material and SMA, all components of the isolator are made of steel. Figure 1 shows a schematic diagram of the developed hybrid isolation device The working principle of the SFB is described as follows: with small external loadings, such as winds or small earthquakes, the SFB can act as a type of stiff link to satisfy the serviceability requirement of the isolated structures. Under moderate and strong ground motions, seismic excitations motivate the sliding mechanism of the SFB, which can reduce the seismic energy transfer across the isolation interface and produce the deformation of the SMA springs. During the mutual movements between the top plate and the bottom plate, the SMA helical springs enhance global energy dissipation capacity of the isolation system and confine displacement of the isolators in the design range. After the earthquakes, the SFB will recover to its original shape as a result of re-centering ability of the superelastic SMA elements.

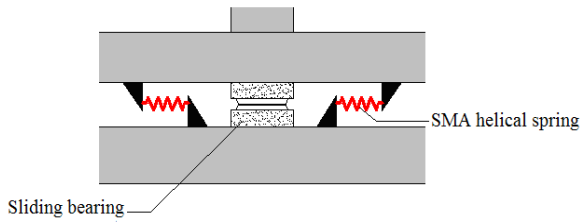

Fig. 1 Schematic diagram of configuration of SFB

Analytical model for SMA helical spring

The SMA helical spring can be modeled using solid finite elements based on the Liang-Rogers model [8], but it is generally impractical for nonlinear time history analysis of a complete engineering structure because of too much time that is required to build and analyze such numerical model. When building an analytical model of a structure controlled by SMA devices, the mechanical behaviors of the structural components are often described with simple hysteretic models that are convenient in practical application.

In this study, the SMA spring is modeled with a combination of two nonlinear elements to simulate superelastic behavior exhibited by the SMA helical spring. The model consists of the following components:

Element I: nonlinear elastic element. This element is used to capture the stiffness property of the SMA spring under cyclic loading-unloading process. The computational model of the element is given by

$$F_{ml} = \begin{cases} \pm K_{s1}|x| & |x| \le x_a \\ \pm\left[K_{s1}x_a + K_{s2}\left(|x| - x_a\right)\right] & x_a < |x| \le x_b \end{cases} \tag{1}$$

where F_{ml} is the restoring force provided by the nonlinear elastic element; x is the displacement of the nonlinear elastic element; x_a is the yield displacement; K_{s1} is the initial stiffness of the nonlinear elastic element computed from following equation

$$K_{s1} = \left(hF_a\right)/x_a$$

where η is the ratio between $F_{ml}(x_a)$ and F_a and can be obtained by trial and adjustment. K_{s2} is the post-yielding stiffness of the nonlinear elastic element calculated by

$$K_{s2} = \left[F_b - (1-h)F_a\right]/\left(x_b - x_a\right)$$

Element II: hysteretic element. This element describes an elasto-plastic behavior with a smooth transition from the elastic to plastic range, which is used to account for the energy dissipation capacity of the SMA spring. The element is based on the Bouc-Wen model [9], and its force-displacement relation can be given as follows

$$F_w = a\frac{F_y}{x_a}x + (1-a)F_y z \tag{2}$$

where F_w is the restoring force provided by the hysteretic element; $F_y = (1-h)F_a$ is the yield force of the hysteretic element; α is the ratio of the post-yielding to elastic stiffness; z is the hysteretic dimensionless quantity expressed as

$$x_a\dot{z} + g|\dot{x}|z|z|^{n-1} + b\dot{x}|z|^n - A\dot{x} = 0 \tag{3}$$

where γ, β, A and n are dimensionless parameters that control the shape of the hysteresis loop.

The nonlinear elastic element and the hysteretic element work in parallel under the same displacement to provide a overall restoring force of the SMA helical spring, which can be computed as

$$F_{SMA} = F_{ml} + F_w \tag{4}$$

where F_{SMA} is the restoring force of the superelastic SMA spring.

In general, the element properties described above can be derived by utilizing the primary parameters for the model proposed by Liang and Rogers. Therefore, it is clear that the existing Liang-Rogers mechanical model can be employed for initial analysis of engineering structures with SMA-based devices, while the developed hysteretic model is used in simulating cyclic response of SMA helical spring in a complete structure.

Mechanical behavior of SMA –based isolator

Analytical model for SFB

The SFB model is an assembly of the SMA helical spring, slider and sliding surface. The restoring force developed in the SFB is given by

$$F_{IS} = F_f + F_{SMA} \tag{5}$$

where F_{IS} denotes the restoring force of the SFB system; F_f represents the frictional force of steel-Teflon sliding bearing. A hysteretic model proposed by Constantinou et al. [10] is used to

simulate the force of the sliding bearing. The frictional force at a flat sliding intersurface is given by

$$F_f = mWz \tag{6}$$

where μ is the coefficient of friction; W represents the normal load carried by the bearing interface; the hysteretic dimensionless quantity z is governed by the follow differential equation

$$Y\dot{z} + g\left|\dot{u}_b\right|z\left|z\right|^{n-1} + b\dot{u}_b\left|z\right|^{n} - A\dot{u}_b = 0 \tag{7}$$

where Y is the yield displacement of the sliding bearing; $\dot{u}_b$ is the slip velocity of the sliding bearing.

The coefficient of friction μ can be expressed as

$$m = m_{max} - Dm\, exp\left(-a_f\left|\dot{u}_b\right|\right) \tag{8}$$

where μ_{max} is the coefficient of friction at very high velocity; $\Delta\mu$ is the difference between the coefficient at very high and very low velocities; a_f is a constant for a given bearing pressure and condition of the sliding interface.

Cyclic response of SFB

SMA helical spring experimental tests

Experimental tests have been performed on superelastic helical spring made from $Ni_{50.8}Ti_{49.2}$ SMA. The tested specimen is characterized by the following geometry: the coil is made of a 12mm diameter superelastic SMA bar. The spring specimen and test machine set-up are shown in Figure 2. The resulting force-displacement curves of the SMA helical spring are obtained (Figure5). As shown in Figure 3, the spring system is characterized by a stable superelastic behavior. After the tests, the initial geometry of the tested spring is perfectly recovered.

Fig. 2 NiTi SMA spring

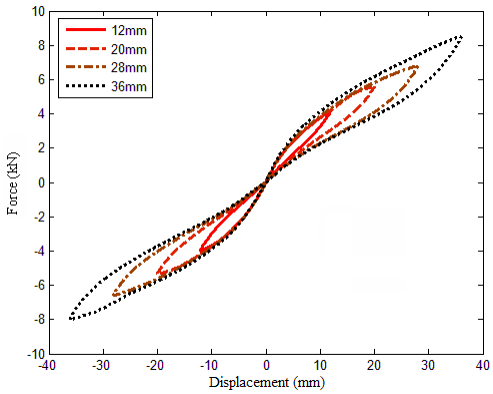

Fig.3 Force-displacement curves of SMA springs

Mechanical experiment of SFB

Using the previously described SMA helical spring, the tested specimen of SFB is designed and fabricated. The isolation device specimen consists of two NiTi SMA helical springs and a steel-Teflon sliding bearing. The details of the SFB specimen are plotted in Figure 4. The experiment is accomplished using an electro-hydraulic loading system. The system mainly consists of three subsystem: the controlling system, the oil hydraulic system and measurement system. Figure 5 gives a photograph of the SFB specimen for experimental tests.

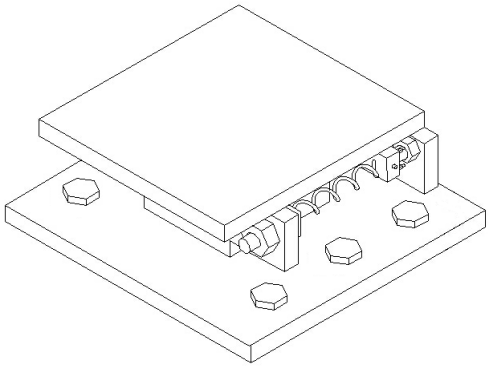

Fig. 4 Three dimensional schematic diagram of SFB

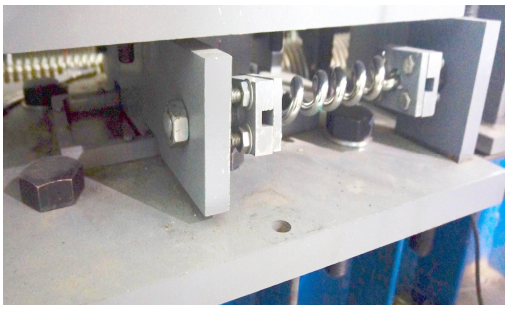

Fig.5 Photo of SFB specimen

The mechanical experiment is conducted using a displacement controlled cyclic loading, and the loading scheme follows a triangular loading pattern with increasing displacement amplitude. Figure 6 presents the typical hysteretic loops of the SFB. As shown in Figure 6, the SFB exhibits stable hysteresis behavior under the cyclic loading with large displacement amplitude. In order to further investigate the property of the new isolator, numerical simulation is carried out by using Matlab software. As for the SMA helical spring, the performance parameters are K_{s1}=0.25kN/mm, K_{s2}=0.16kN/mm, x_a=5.0mm, F_y=1.2kN, α=0, β=0.5, γ=0.5, A=1 and n=1. The performance parameters for the frictional force at a sliding interface are Y=0.5mm, μ_{max}=0.095, $\Delta\mu$=0.02 and a_f=0.02s/mm. The hysteresis loops of the SFB specimen obtained from the simulation and the experiment are both plotted in Figure 7. It is shown that good agreement is achieved between the theoretical and the measured results.

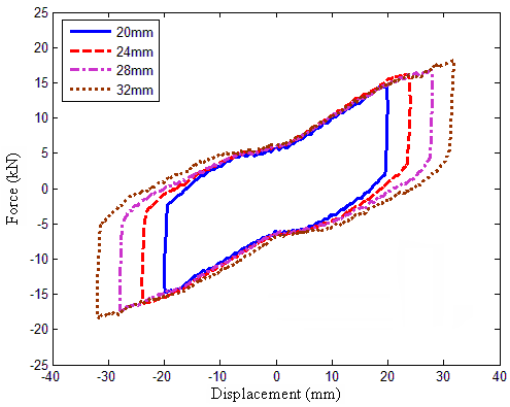

Fig. 6 Hysteretic loops of the SFB

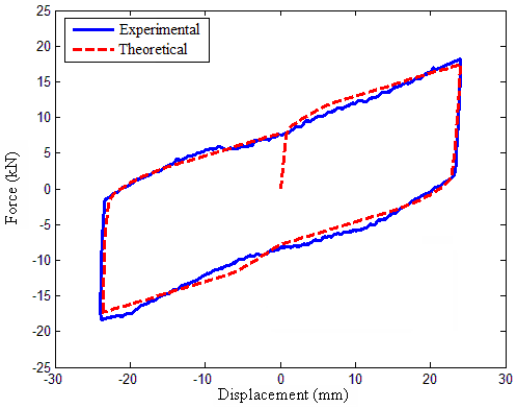

Fig. 7 Experimental and theoretical hysteretic loops

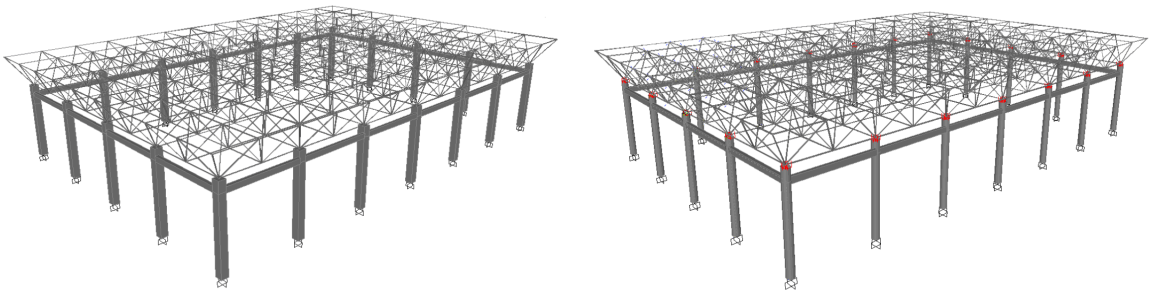

(a) Non-isolated structure (b) Isolated structure

Fig. 8 Finite element models of spherical lattice shells

Analysis of the double-layer lattice shell structure with SFB

Structural Model

The finite element model of the lattice grid structure is shown in Figure 8, where the roof is supported by steel columns through SFB devices. The lattice grid roof has a span of 48m. The thickness between upper and lower chords is taken as 2m. Several types of steel tubes, f140×8, f180×8, are selected as the members of the lattice grid structure, which are modeled as bar elements in the analysis. Under the lattice shell and the steel box beam, f500×16 steel columns are available for supporting the lattice grid roof. In this study, SAP2000 software is applied to model and calculate the dynamic response of structure. The roof load is taken as 0.7kN/m^2. All the loads and self-weight of the structure are treated as lumped masses concentrated at the nodes of the structure. Three kinds of nonlinear element, the nonlinear elastic element, Wen plastic element and friction isolator element, are employed to simulate the SFB in the SAP2000 software. These nonlinear elements are combined to reproduce the mechanical behavior the proposed SFB device. The performance parameters of the tested SFB specimen are utilized to establish the structural model. The El-Centro wave, Taft wave, Northridge wave, Petrolia wave are selected as seismic inputs in X-directions. Their PGAs are adjusted to 400cm/s^2, and their duration times are all set to 40s. In the analysis, two supporting conditions, i.e., hinged support and SFB devices are considered in order to compare seismic performance.

Seismic response

Seismic response analyses are performed for the lattice grid structures under the conditions with and without SFB devices, from which seismic responses of both the structure and the bearing device have been obtained. Figure 9 shows acceleration response of node obtained from the time history analyses. Table 1 gives residual displacement of SFB. Peak base shear is shown in Figure 10. The

displacement time histories of the SFB are shown in Figure 11. Numerical results show that the response of the roof and the substructure are significantly suppressed with the use of SFB. Figure 12 shows the hysteresis loops of such an isolation device under seismic excitations. Note that the SFB has a good energy dissipation performance and re-centering capability in controlling bearing displacement, which is very important for the seismic protection of lattice shell structures with passive isolation bearing devices.

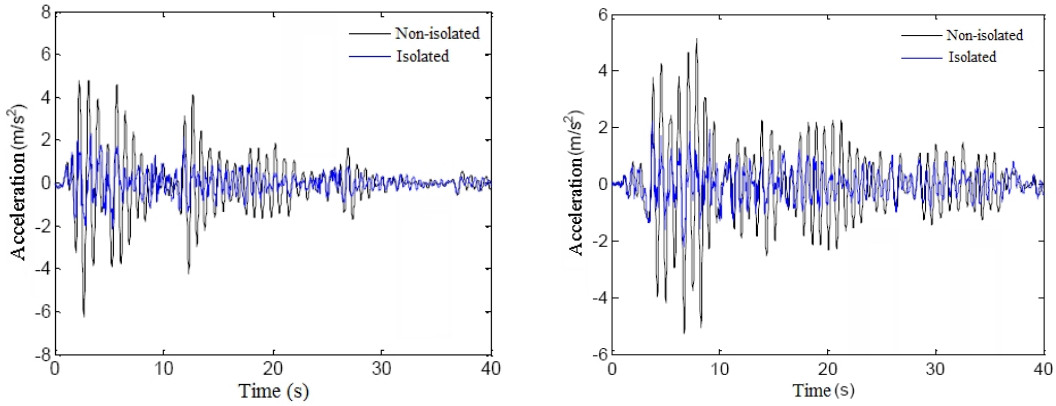

(a) El-centro wave (b) Taft wave

Fig. 9 Time histories of acceleration of node

Table 1 Residual displacement of SFB

Earthquake records	El-Centro	Tafr	Northridge	Petrolia
Residual displacement(mm)	2.3	2.7	1.5	1.8

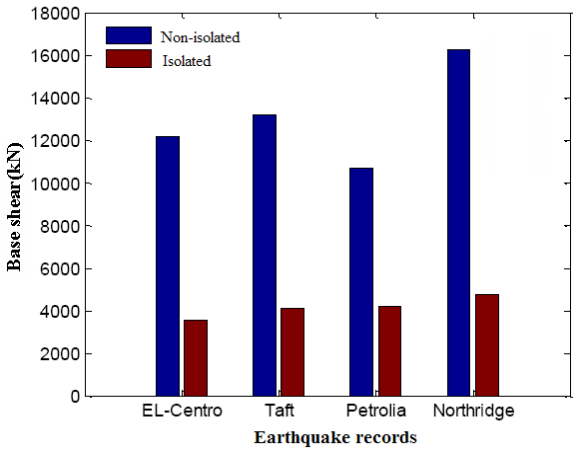

Fig.10 Peak base shear of structures

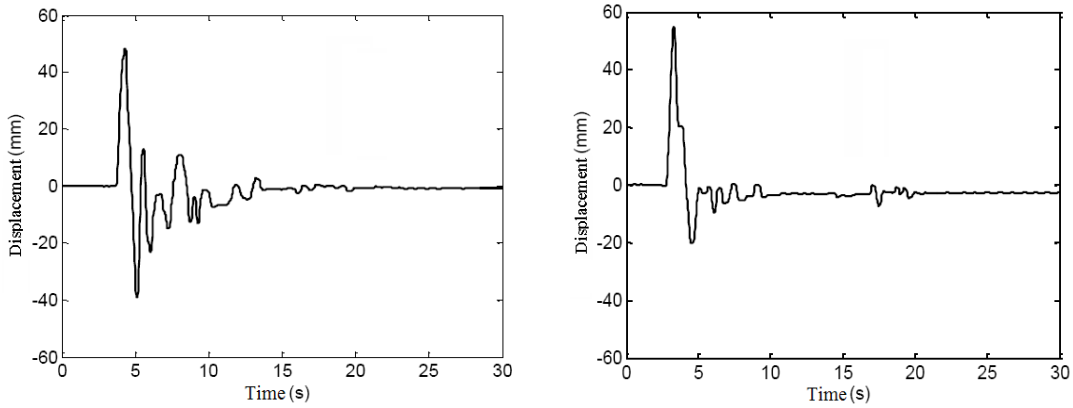

(a) Northridge wave (b) Petrolia wave

Fig. 11 Time histories of displacement of SFB

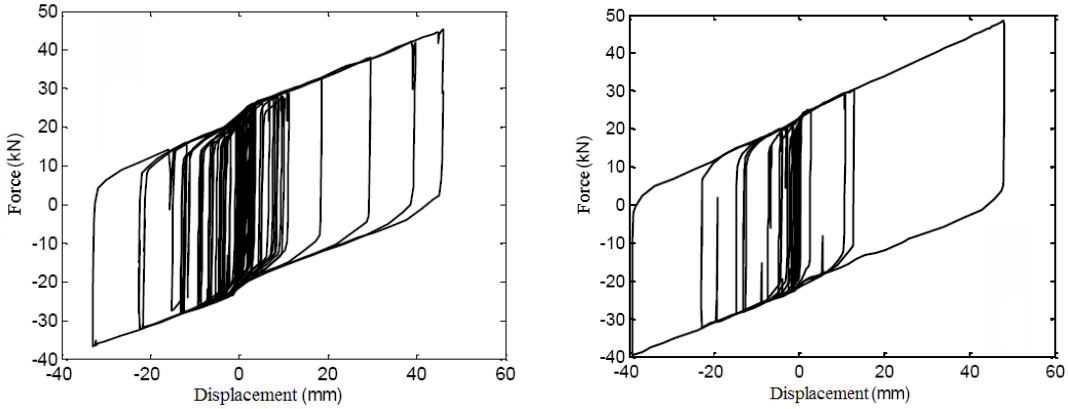

(a) El-Centro wave (b) Northridge wave

Fig. 12 Hysteresis loops of the SFB

Conclusions

In this paper, the theoretical model and experimental tests of the SFB are investigated. The feasibility of using the SFB in the seismic isolation of a lattice structure is discussed. From the experimental and numerical studies, the following conclusions can be obtained:

(1) The proposed SFB utilizing sliding friction and superelasticity provides satisfactory energy capacity and re-centering property.

(2) The results of mechanical experiment show good agreement with the results of the numerical simulation.

(3) The seismic responses of the lattice grid structure can be effectively reduced using the SFB, and the sliding displacements of the SMA-based isolators are adequately controlled, which is of great significance in practical engineering applications.

Acknowledgement

The authors gratefully acknowledge the support from Beijing Natural Science Foundation (Grant No. 8132024).

References

[1] Graesser E, Cozzarelli F. Shape memory alloys as new materials for aseismic isolation. Journal of Engineering Mechanics, 1991; 117; 2590-2608.

[2] Dolce M, Cardone D, Marnetto R. Implementation and testing of passive control devices based on shape memory alloys. Earthquake Engnineering and Structural Dynamics, 2000; 29; 945-968.

[3] Dolce M, Cardone D, Ponzo F, et al. Shaking table tests on reinforced concrete frames without and with passive control systems. Earthquake Engnineering and Structural Dynamics, 2005; 34; 1687-1717.

[4] Ozbulut O, Hurlebaus S. Optimal design of superelastic-friction base isolators for seismic protection of highway bridges against near-field earthquakes. Earthquake Engineering and Structural Dynamics, 2011; 40; 273-291.

[5] Bhuiyan A, Alam M. Seismic vulnerability assessment of a multi-span continuous highway bridge fitted with shape memory alloy bars and laminated rubber bearing. Earthquake Spectra, 2012, 28 (4): 1379-1404.

[6] Speicher M, Hodgon D, DesRoches R, et al. Shape memory alloy tension/compression device

for seismic retrofit of buildings. Journal of Material Engineering and Performance, 2009; 18; 746-753.
[7] Attanasi G, Auricchio F, Urbano M. Theoretical and experimental investigation on SMA superelastic springs. Journal of Materials Engineering and Performance, 2011; 20; 706-711.
[8] Liang C, Rogers C. Shape memory alloy spring with applications in vibration control. Journal of Vibration and Acoustics, 1993; 115; 129-135.
[9] Wen Y K. Method for random vibration of hysteretic system. Journal of the Engineering Mechanics Division, 1976; 102; 249-263.
[10] Constantinou M, Mokha A, Reinhorn A. Teflon bearing in base isolation II: modeling. Journal of Structural Engineering, 1990; 116; 455-474.